Soft X-ray Activated Lanthanide Scintillator for Controllable NO Release and Gas-Sensitized Cancer Therapy

Mingyang Jiang, Zhenluan Xue,Youbin Li, Hongrong Liu, Songjun Zeng, and Jianhua Hao**

Prof. S. J. Zeng, Dr. M. Y. Jiang, Z. L. Xue, Y. B. Li, and H. R. Liu,

College of Physics and Information Science and Key Laboratory of Low-dimensional Quantum Structures and Quantum Control of the Ministry of Education, Synergetic Innovation Center for Quantum Effects and Applications, Hunan Normal University, Changsha, Hunan 410081 (China)

E-mail: ***songjunz@hunnu.edu.cn***

Prof. J. H. Hao

Department of Applied Physics, The Hong Kong Polytechnic University, Hong Kong (China)

E-mail: ***jh.hao@polyu.edu.hk***

Keywords: Lanthanide scintillator; radioluminescence; soft X-ray triggered NO release; gaseous therapy

Abstract:

Multifunctional light stimuli-responsive NO-based gaseous theranostic systems are highly desirable due to the direct1y ki11ing cancer ce11s at high concentration (>1 μM) with minimized adverse effects. However, on-demand NO-releasing nano-platform for deep-tissue gas-based cancer therapy has not yet been explored. Herein, we develop a new type of soft X-ray-activated $NaYF_4$:Gd/Tb scintillator as light transducer for depth-independent NO release and on-demand gas-sensitized cancer therapy. Benefiting from excellent radioluminescent property of $NaYF_4$:Gd/Tb, deep-tissue (up to 3 cm) NO release can be achieved by ultralow dosage soft X-ray (45 kVp, 0.18-0.85 mGy) irradiation. More importantly, the designed scintillator-based NO gasotransmitter presents significant inhibition of tumor growth under ultralow dosage soft X-ray irradiation. Therefore, such soft X-ray activated NO-releasing nanoplatform provides a promising depth-independent gaseous therapy mode for defeating deep-seated cancer in the future.

1. Introduction

The development of theranostic systems based on endogenous gas has been emerged as new green treatment paradigm and opens up new frontiers for carcinoma therapy due to its non-invasive nature and great benefits to metabolism[1]. As a new gaseous therapeutic molecule, nitric oxide (NO) plays a key role in various biological process including neuronal communication regulation, blood vessel modulation, and other physiological/pathophysiological activities[2]. Recent reports[3-5] revealed that NO presented a concentration-dependent dual effect for promotion or inhibition of tumor. At low concentration (1 pM - 1 nM), NO has a promoting effect on tumor growth. In contrast, high concentration of NO (>1.0 μM) may remarkably inhibit tumor growth[3-5]. Therefore, developing stimuli-responsive NO releasing system with precisely controlled NO generating concentration for on-demand cancer therapy with little systemic toxicity is urgently demanded.

In response to this issue, some NO releasing systems for controllable generation of NO by certain stimuli, including heat[6], PH[7], or light[8] were well-developed. Among these systems, photo-triggered NO releasing platforms were emerged as the promising NO-releasing transducer due to the precise control of timing, location, and dosage[9]. While, most of photoactive NO-releasing molecules, such as Metal-NO compounds (Roussin's black salt, RBS), nitroimines and bis-N-nitroso complexes only respond to ultraviolet (UV) and visible light[10]. However, the low penetration depth in tissue of UV/visible light greatly impedes their further application for controllable NO release *in vivo*. In contrast to UV/visible light, near-infrared (NIR) light located in the "optical transparency window" (700-900 nm) has been considered as an alternative stimuli light source for *in vivo* NO release owing to the improved tissue penetration depth[11] Recently,

upconversion (UC) luminescent nanomaterials[12] capable of converting low energy photon (NIR light) to high energy UV/visible light through frequency UC process were emerged as promising NIR light-sensitive sensor[8b, 13] for NO releasing. While, the low UC luminescent quantum yield and relative low penetration depth of NIR light still hinder their deep-tissue gas-based therapy of tumor. In comparison to visible and NIR light, X-ray photons with greatly increased penetration depth in tissues have been widely applied in diagnosis and radiotherapy for clinical, especially for X-ray activated radioluminescence[14].

Therefore, developing the X-ray activated NO-releasing system is highly desirable for deep-tissue on-demand NO release. Recently, Shi and his co-workers demonstrated a pioneering study for X-ray-induced NO-release by using high energy X-ray to break down S-N bonds[15]. Nevertheless, high-dosage X-rays (>5.0 Gy) were required in this system, which inevitably caused side effects to normal tissues[16]. In this regard, we propose a scintillating nanomaterial as the energy transducer to convert the low dosage X-ray photons to visible light, and further activate the surrounding photoactive NO donors for generating NO gas.

Herein, a lanthanide-based scintillating nanomaterial ($NaYF_4$:Gd/Tb nanorod) as the energy transducer (Scheme 1) for controllable NO release was explored. Owing to the efficient conversion of X-ray photons to visible light, when absorbing RBS molecule, the designed scintillator presented soft X-ray triggered on-demand NO release under ultralow dosage (0.18-0.85 mGy) of X-ray irradiation via energy transfer (ET) from scintillator to RBS. Additionally, deep tissue NO release up to 3 cm was also achieved, which broke the major challenge of the depth barrier suffered by the traditional UV/visible and NIR light. More importantly, *in vivo* gas-sensitized tumor therapy was

successfully performed, demonstrating directly inhibition of tumor growth.

2. Results and Discussion

2.1 Construction of $NaYF_4$:Gd/Tb-RBS nanocomposites

For exploring the soft X-ray activated NO-releasing system, the silica coated $NaYF_4$: 40%Gd/15%Tb rare-earth (RE) nanorods were used for absorbing $[Fe_4S_3(NO)_7]^-$ (RBS) NO-donor via electrostatic interaction (Figure 1a). Firstly, hexagonal phase $NaYF_4$:Gd/Tb nanorods with uniform rod-like morphology (Figure 1b,c) were prepared using a hydrothermal method by doping Gd^{3+}. The interplanar distance was measured to be 2.95 Å via the high resolution transmission electron microscopy (HR-TEM) image (Figure 1d), corresponding to the (110) crystal plane of the hexagonal-phase $NaYF_4$. The X-ray diffraction (XRD) results indicated that all the diffraction peaks were well indexed to the hexagonal phase structure (JCPDS No. 16-0334) and no impurities were detected (Figure 1h). Then, a silica layer with thickness of about 10 nm was coated on $NaYF_4$: Gd/Tb nanorods, which not only transferred the hydrophobic nanorods to water phase, but also provided the ability to absorb the RBS molecules. As shown in Figure 1e and 1f, the TEM results provided the evidence of the formation of $NaYF_4$:Gd/Tb@SiO_2 core-shell structure. Then, $NaYF_4$:Gd/Tb@SiO_2 nanocomposites were modified with 3-aminopropyltriethoxysilane (APTES) to form $-NH_3^+$ group on the surface, and finally reacted with RBS to form $NaYF_4$:Gd/Tb@SiO_2-RBS (hereafter referred to as $NaYF_4$:Gd/Tb-RBS) nanocomposites via electrostatic interaction. Previous report[8b] have demonstrated that RBS can release NO due to the photolysis effect under UV/visible light irradiation. And as demonstrated in Figure 1i, the emission spectrum of $NaYF_4$:Gd/Tb nanorods was nicely overlapped with the broad-band absorption region

of the RBS, leading to the occurrence of ET from lanthanide nanorods to RBS.

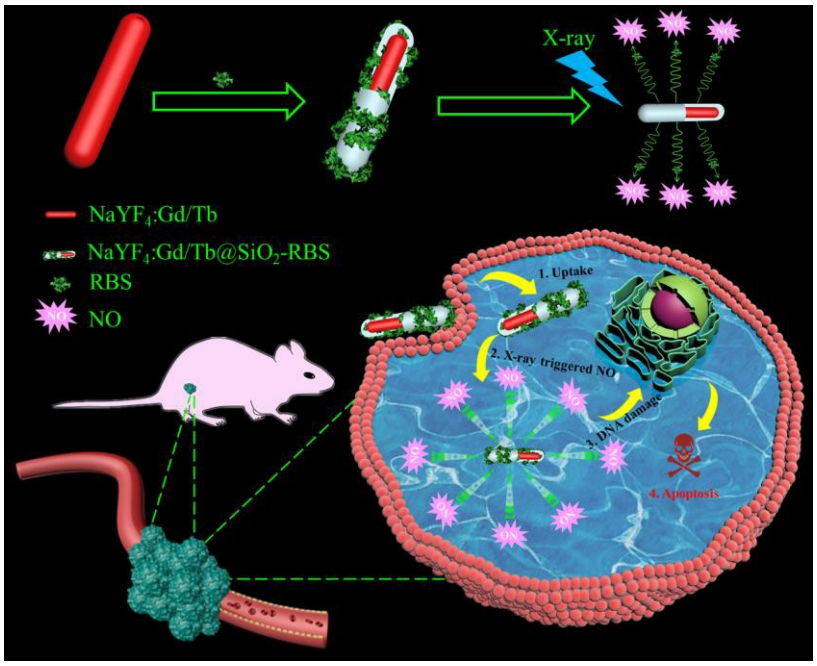

Scheme 1. Schematic illustration of designing $NaYF_4$:Gd/Tb-RBS nanocomposites for ultralow dosage soft X-ray triggered NO release.

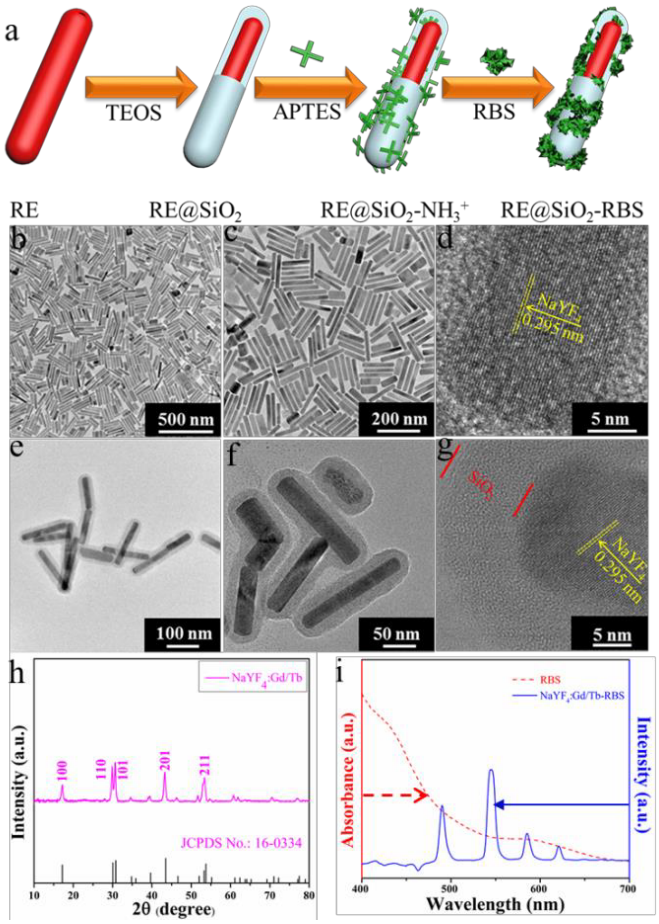

Figure 1. a) Schematic illustration of the synthesis of the $NaYF_4$:Gd/Tb-RBS nanocomposites. b-c) TEM images of $NaYF_4$:Gd/Tb nanorods. d) HR-TEM image of a single $NaYF_4$:Gd/Tb nanorod. e-f) TEM images of $NaYF_4$:Gd/Tb@SiO_2 nanorods. g) HR-TEM image of a single $NaYF_4$:Gd/Tb@SiO_2 nanorod. h) XRD pattern of $NaYF_4$:Gd/Tb nanorods. bottom: the standard pattern for hexagonal phase $NaYF_4$. (JCPDS No. 16-0334). i) UV/Vis absorption spectra of RBS aqueous solution and the emission spectrum of $NaYF_4$:Gd/Tb@SiO_2 nanorods under the excitation of UV light.

2.2 Soft X-ray triggered radioluminescence of $NaYF_4$:Gd/Tb@SiO_2 scintillator

To demonstrate the ability of $NaYF_4$:Gd/Tb@SiO_2 nanorods as soft X-ray stimuli-responsive

NO release, the *in vitro* soft X-ray induced visible light emitting experiments were first carried out. A series of 96-well tubes containing different concentrations of $NaYF_4$:Gd/Tb@SiO_2 were used for green radioluminescence test under soft X-ray irradiation with low dosage (Table S1). Figure 2a showed that the green emission signals were significantly increased with increasing the concentrations of $NaYF_4$:Gd/Tb@SiO_2. In addition, the radioluminescent signals of the same samples were also greatly enhanced by improving the X-ray tube voltage. As illustrated in Figure 2b, the average radioluminescent intensity visually confirmed that high tube voltage promoted the X-ray-induced green emission. To further reveal the irradiation time-dependent radioluminescent properties, $NaYF_4$:Gd/Tb@SiO_2 samples were irradiated with different irradiation times from 1 to 4 min under the same X-ray tube voltage of 45 kVp. As demonstrated in Figure 2c, long irradiation time was highly desirable for achieving the intense radioluminescence, which was also vividly presented in the average intensity distribution diagram (Figure 2d). Moreover, covered with different thicknesses of pork slabs (0-3 cm), the radioluminescent signals were still observed, even up to 3 cm depth, indicating the depth-independent behaviors of X-ray light source (Figure S1). To further examine the capability of $NaYF_4$:Gd/Tb@SiO_2 for *in vivo* X-ray induced optical imaging, $NaYF_4$:Gd/Tb@SiO_2 solution (150 μL, 2 mg/mL) was subcutaneously injected into a mouse. As shown in Figure S2a,b, significant signals were observed in the treated mouse. And the signal intensity was increased with improving the X-ray tube voltage, indicating the feasibility of the designed scintillating nanomaterials for *in vivo* X-ray induced optical imaging. Therefore, these findings demonstrate that $NaYF_4$:Gd/Tb@SiO_2 presents high efficient radioluminescence under low dosage soft X-ray activation, which can be used as promising light-responsive transducer for NO

release under low dosage soft X-ray irradiation.

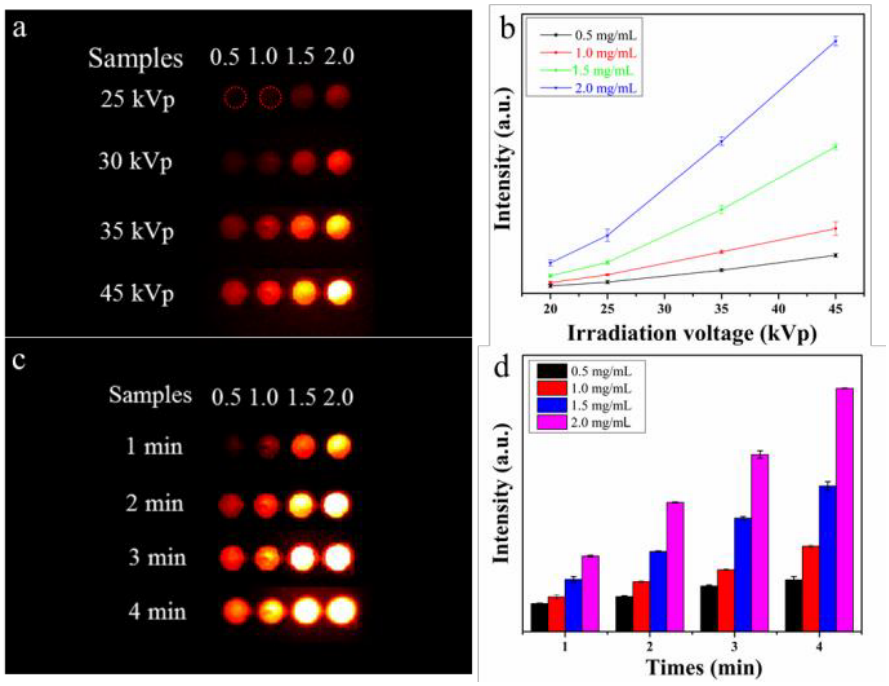

Figure 2. a) Soft X-ray induced optical imaging with different concentrations of $NaYF_4$:Gd/Tb@SiO_2 solutions under different X-ray tube voltages and same irradiation time of 2 min. b) The corresponding average signal intensity under different tube voltages. c) X-ray induced optical imaging under different irradiation times and same tube voltage of 45 kVp. d) The corresponding average signal intensity.

2.3 Soft X-ray triggered NO release

Owing to the significant X-ray induced green radioluminescence and spectra overlap between $NaYF_4$:Gd/Tb and RBS, soft X-ray triggered NO release can be readily achieved via ET from $NaYF_4$:Gd/Tb nanorods to RBS (Figure 3a). In order to verify the soft X-ray triggered NO release, the NO releasing properties of the different solutions containing deionized water, $NaYF_4$:Gd/Tb@SiO_2, and $NaYF_4$:Gd/Tb-RBS were studied by using a typical Griess assay[17]. As

shown in Figure 3b,c, there is nearly no NO generation from deionized water and $NaYF_4$:Gd/Tb@SiO_2 solution when irradiated under different X-ray tube voltages from 0 to 45 kVp with irradiation time of 4.5 min. While, the designed $NaYF_4$:Gd/Tb-RBS (Figure 3d) presents obvious soft X-ray triggered NO release and the release rate increases by improving the X-ray tube voltage. In addition, the quantitative NO release concentrations from RBS and $NaYF_4$:Gd/Tb-RBS were further studied under the soft X-ray irradiation with different tube voltages and irradiation times. As demonstrated in Figure 3e, the X-ray triggered NO release content from 3.7 μM - 6.4 μM could be achieved by adjusting X-ray tube voltage from 25 kVp to 45 kVp, which was mainly ascribed to the efficient ET from $NaYF_4$:Gd/Tb nanorods to RBS molecules. The absorption spectra (Figure 3f) of $NaYF_4$:Gd/Tb-RBS + Griess kit were further tested and presented the enhancement of absorption value with increasing soft X-ray irradiation times, further verifying the soft X-ray activated NO release. More importantly, controllable gas release plays an important role in realizing on-demand gas-sensitized therapy. Then, the precisely controllable NO release triggered by soft X-ray was further investigated. As demonstrated in Figure 3g, with continuous irradiation for 30 s, a burst NO release was initiated at this stage. Then after stopping X-ray irradiation for 1 min, the NO release rate is greatly decreased, indicating the on-demand NO release by utilizing intermittent X-ray irradiation.

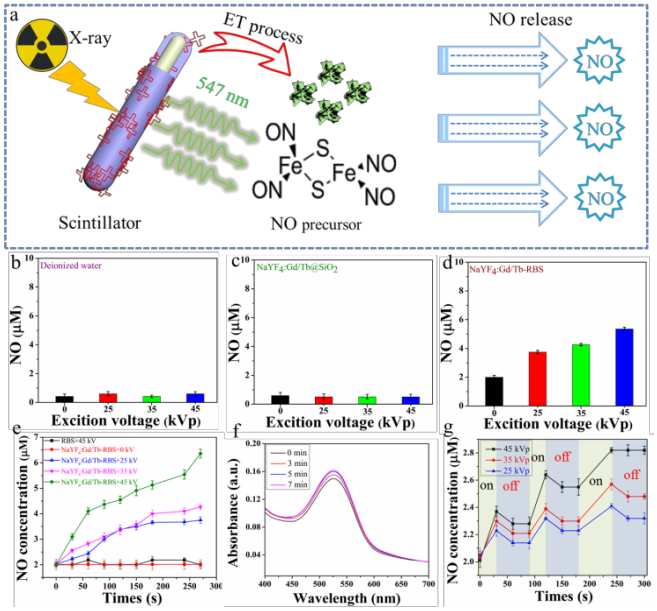

Figure 3. a) Schematic diagram of the NO releasing mechanism induced by soft X-ray. b-d) Quantitative soft X-ray induced NO release from deionized water, $NaYF_4$:Gd/Tb@SiO_2, and $NaYF_4$:Gd/Tb-RBS. e) NO-releasing curves of $NaYF_4$:Gd/Tb-RBS and RBS triggered by different tube voltages of X-ray and irradiation times. f) UV/Visible absorption spectra of $NaYF_4$:Gd/Tb-RBS + Griess kit solution under 45 kVp X-ray irradiation with different irradiation times. g) On-demand NO-releasing behaviour induced by X-ray irradiation.

In addition, deep tissue NO release is another key factor for gas-sensitive tumor therapy in biomedicine application. To reveal the deep tissue NO releasing nature, X-ray triggered NO releasing properties of the designed $NaYF_4$:Gd/Tb-RBS system covered with various thicknesses of pork slices from 0 to 3 cm were further studied (Figure S3). With soft X-ray irradiation for 30 s at 45 kVp, the designed $NaYF_4$:Gd/Tb-RBS sample covered with/without pork slap can sustainably release NO gas under X-ray irradiation, and the releasing content increases with increasing the irradiation time. It is worth noting that the release amount of NO can also reach about 1.5 μM

(Figure S3b) at 3 cm deep tissue after 270 s irradiation, which is higher than the concentration (> 1 μM) for directly killing cancer cells. Therefore, the designed scintillator-based X-ray activated NO releasing system can break through the limitation of penetration depth, promoting deep-tissue gas-sensitized cancer therapy *in vivo*.

It also should be pointed out that low dosage of X-ray is a crucial factor for X-ray induced nanomedicine in clinical application. In our designed scintillator-based NO-releasing gasotransmitter, only ultralow dosage of X-ray (~0.85 mGy, Table S1) is required for soft X-ray activatable NO release, which was far lower than the clinically used X-ray dosage for cancer treatment[18] and previously reported high energy X-ray (>5.0 Gy) induced NO release[15].

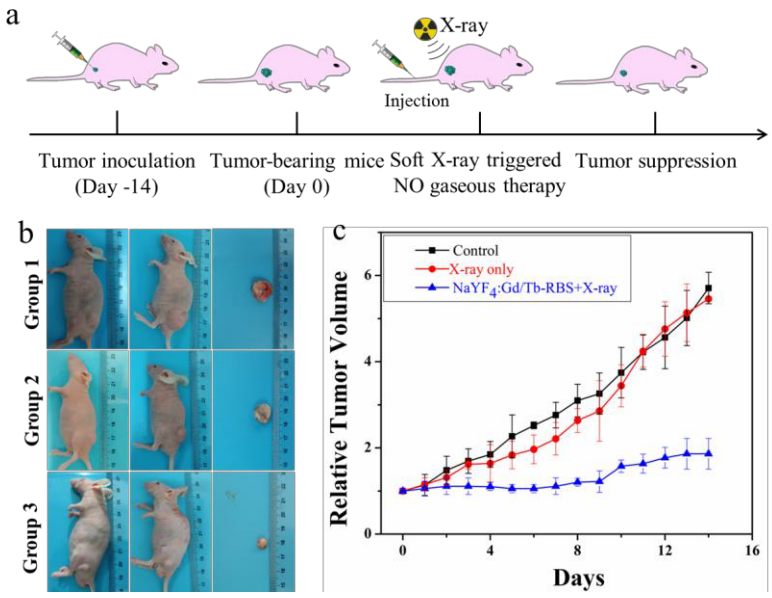

Figure 4. a) Schematic diagram of soft X-ray induced NO-based gaseous therapy of cancer *in vivo*. b) Photographs of tumor-bearing mice before and after treatment. c) The relative volume changes of tumor from control, RBS+X-ray, and $NaYF_4$:Gd/Tb-RBS + X-ray groups.

2.4 NO gas-sensitized tumor therapy

Prior to *in vivo* therapy, the biotoxicity of $NaYF_4$:Gd/Tb-RBS nanocomposites was first studied. The major organs including heart, liver, spleen, lung, and kidney separated from the mice treated with $NaYF_4$:Gd/Tb-RBS nanocomposites were analyzed by hematoxylin and eosin (H&E) staining analysis. As shown in Figure S4, compared with the control group, no obvious histopathological abnormalities or lesions in organs from $NaYF_4$:Gd/Tb-RBS treated group were observed, suggesting the negligible biotoxicity and high biocompatibility. Then, to reveal *in vivo* NO gas-sensitized tumor therapy triggered by ultralow dosage soft X-ray, the Lewis lung cell (LLC) tumor-bearing mice were randomly divided into three groups: control (group 1); RBS + soft X-ray irradiation (group 2); $NaYF_4$:Gd/Tb-RBS + soft X-ray irradiation (group 3). After injection of RBS and $NaYF_4$:Gd/Tb-RBS solution (2 mg/mL, 150 μL), tumors were irradiated by soft X-ray with 45 kVp for 2 min. As shown in Figure 4, the tumors in group 1 and group 2 grow fast, indicating that only low dosage X-ray irradiation shows low efficiency tumor inhibition. In contrast, the combination of $NaYF_4$:Gd/Tb-RBS solution and X-ray irradiation in group 3 presents the remarkable inhibition of tumor growth, which is mainly attributed to the soft X-ray induced NO release for directly killing tumor.

3. Conclusions

In summary, the soft X-ray inducible scintillator-based NO generating nanoplatform by integrating $NaYF_4$:Gd/Tb nanorods with NO donor (RBS) was developed for the first time. On the basis of ET process between $NaYF_4$:Gd/Tb nanorods and NO donor (RBS), ultralow dosage soft X-ray (0.85 mGy) triggered NO release could be achieved in deep tissues even up to 3 cm depth, breaking the depth limitation suffered by the traditional UV/visible and NIR light. By adjusting tube

voltage of X-ray, on-demand NO release was also realized, which was important for concentration-dependent NO gas therapy. Moreover, the X-ray activated $NaYF_4$:Gd/Tb-RBS agent exhibits efficient inhibition effect for tumor growth. These findings open up the opportunity for developing the new type of soft X-ray activatable gasotransmitter for deep tissue gas-sensitized tumor therapy *in vivo*.

4. Experimental Section

Materials: $GdCl_3$ $_2O$ (99.99%), YCl_3 $_2O$ (99.99%), and $TbCl_3$ $_2O$ (99.9%) were purchased from QingDa elaborate Chemical Reagent Co. Ltd (Shandong). NaOH (98%), NaF (99%), oleic acid (OA,90%), absolute ethanol, Igepal CO-520, Tetraethyl orthosilicate (TEOS), 3-aminopropyltriethoxysilane (APTES), iron(II) sulfate heptahydrate ($FeSO_4$ 7 $_2O$, 98%), sodium nitrite ($NaNO_2$, 97%), ammonium sulfide ($(NH_4)_2S$, 48%),ammonium hydroxide (NH_4OH, 33% NH_3) and other reagents were purchased from Sinopharm Chemical Reagent Co., China.

Characterizations: Powder X-ray diffraction (XRD) measurements were performed by a Rigaku D/max 2500 X-ray diffractometer with Cu-Ka radiation (A= 0.1540 nm) at 40 kV and 250 mA. The shape and structure of $NaYF_4$:Gd/Tb and $NaYF_4$:Gd/Tb@SiO_2 samples were characterized by transmission electron microscopy (TEM, FEI Tecnai F20), and high-resolution TEM (HR-TEM) at an acceleration voltage of 200 kV. Photoluminescence spectra of these samples were detected by using a Zolix Analytical Instrument (fluoroSENS 9000 A) at room temperature. The UV-Vis absorption data was acquired by Spectrophotometer system (UV-1800, Hunan Sino-Jewell Electronics Co., Ltd.).

Synthesis of $NaYF_4$:Gd/Tb nanorods: The Ln (40%Gd, 15%Tb) co-doped $NaYF_4$ nanorods were synthesized by a traditional hydro-thermal procedure[19] as follows: Firstly, 1.2 g of NaOH completely dissolved in 2 mL of deionized water under stirring. Then, 10 mL anhydrous alcohol and 20 mL OA were added into the above solution stirring for another 20 minutes. After that, A total of 1 mmol $RECl_3$ (RE = Y, Gd, Tb) at designed concentrations/molar ratios and 8 mL of NaF aqueous solution (1.0 M) were added into the aforementioned solution with vigorously stirring. Subsequently, the mixtures were transferred into a stainless Teflon-lined autoclave (50 mL) and maintained at 190 ℃ for 24 h. The resulting products were washed with ethanol and deionized water.

Synthesis of $NaYF_4$:Gd/Tb@SiO_2-NH_3^+: Firstly, $NaYF_4$:Gd/Tb@SiO_2 core-shell nanocomposites were synthesized according to the previous report.[20] 0.2 mmol $NaYF_4$:Gd/Tb nanorods and 0.1 mL Igepal CO-520 were mixed in 50 mL cyclohexane under stirring for 10 min. Then, 0.8 mL of concentrated ammonia and 0.4 mL Igepal CO-520 were added in above solution and sonicated for 20 min. After that, 0.6 mL TEOS was added drop by drop, and the mixture was stirred for 2 days to obtain $NaYF_4$:Gd/Tb @SiO_2 nanorods. Then, 0.15 mL APTES was added in the mixed solution under stirring for 24 h. The resulting $NaYF_4$:Gd/Tb @SiO_2 products were washed with ethanol several times and finally dispersed in 5 mL deionized water.

Synthesis of RBS: RBS was synthesized as following[21]: First, the 8 mL deionized water containing 1.8 g $NaNO_2$ was added to 250 mL 3-neck flask. Then, 2 mL $(NH_4)_2S$ solution and 6 mL of deionized water were added into the above solution. The yellow solution was heated at reflux under stirred until the mixed solution turned to a deep red. Then, 32 mL deionized water containing

4.0 g $FeSO_4$ 7 $_2O$ was added to the above solution. After 30 s heating, 10 mL of a 22% NH_4OH solution was dropped into the mixed solution. The solution was heated to 90 C for 10 min and then filtered immediately. The red-brown Fe $(OH)_3$ was discarded, and the black-brown solution was allowed to stand overnight. The black-brown solution was kept in 4 C overnight and the black crystalline solid was collected and freeze-dried.

Synthesis of RBS-loaded NaYF₄:Tb@SiO₂: $NaYF_4$:Gd/Tb@SiO_2-RBS nanocomposites were synthesized according to an electrostatic attraction procedure. An aqueous solution of RBS (100 mg) was dropwisely added into the suspension of $NaYF_4$:Gd/Tb@SiO_2 (0.2 mmol) under stirring. After 12 h, the precipitate was obtained by centrifugation at 6,000 rpm. Nanocrystals were centrifuged and washed with water three times.

In vitro low dose X-ray induced green emission: Soft X-ray induced green emission was carried out by a multi-modal *in vivo* imaging system (Bruker *In Vivo* FX Pro) equipped with a detecting CCD (ML4002, Finger Lakes Instrumentation, USA). Different concentrations of $NaYF_4$:Gd/Tb@SiO_2 nanorods (0.5 mg/mL, 1.0 mg/mL, 1.5 mg/mL, 2.0 mg/mL) were transferred into 96-well tubes for X-ray induced optical bioimaging with various irradiation times (1-4 min) and excitation tube voltages (25 -45 kVp).

Tumor animal models: 8×10^6 Lewis lung cancer (LLC) cells were subcutaneously injected into BALB/c nude mice, after further culturing about two weeks, the tumor-bearing mouse models were obtained for *in vivo* soft X-ray-activated NO gas therapy experiments. All animal procedures in this study were performed in accordance with the Guidelines for Care and Use of Laboratory Animal

Center of Hunan Normal University and approved by the Animal Ethics Committee of Hunan Province.

In vivo low dose X-ray activated optical bioimaging: $NaYF_4$:Gd/Tb@SiO_2 (150 μL, 2 mg/mL) was then subcutaneously injected in Kunming mouse which was anesthetized by intraperitoneally injecting pentobarbital sodium aqueous solution (10 wt%, 100 μL), After that, a multi-modal *in vivo* imaging system was used for soft X-ray induced bioimaging under X-ray (45 kVp, 2 min) irradiation at room temperature.

Measurement of NO release in deionized water: The NO release contents from $NaYF_4$:Gd/Tb -RBS nanocomposites were quantitatively measured by a classic Griess reagent Kit[17]. When in contact with water, the released NO molecules could be converted into nitrate and/or nitrite. After reaction with the Griess agent, the nitrate and nitrite were finally converted into an azo dye that could be quantitatively determined using a microplate reader or UV-vis absorption spectroscopy (A= 540 nm).

Soft X-ray-activated NO gas therapy: The tumor-bearing mice were randomly into 3 groups: control (group 1); RBS+ X-ray irradiation (group 2); $NaYF_4$:Gd/Tb-RBS + X-ray irradiation (group 3). After injection of RBS and $NaYF_4$:Gd/Tb-RBS solution (2 mg/mL, 150 μL), tumors were irradiated by soft X-ray with 45 kVp for 2 min every day.

Histology analysis: To obtain histology analysis, the main organs including heart, liver, spleen, lung and kidney from the control and treated mice with 3 and 7 days were collected for hematoxylin and eosin (H&E) staining to examine the potential toxicity.

Supporting Information

Supporting Information is available from the Wiley Online Library or from the author.

Acknowledgment

This work was supported by the National Natural Science Foundation of China (No. 21671064), Science and Technology Planning Project of Hunan Province (No. 2017RS3031) and the Hunan Provincial Innovation Foundation for Postgraduate (CX2017B223).

References

[1] Y. Qian, J. B. Matson, *Adv. Drug Deliver. Rev.* **2017**, *110*, 137.

[2] a) K. R. Vega-Villa, J. K. Takemoto, J. A. Yanez, C. M. Remsberg, M. L. Forrest, N. M. Davies, *Adv. Drug Deliver.* Rev. **2008**, *60*, 929; b) B. Fadeel, A. E. Garcia-Bennett, *Adv. Drug Deliver. Rev.* **2010**, *62*, 362; c) W. P. Fan, B. C. Yung, X. Y. Chen, *Angew. Chem. Int. Ed.* **2018**, *57*, 8383.

[3] a) W. M. Xu, L. Z. Liu, M. Loizidou, M. Ahmed, I. G. Charles, *Cell Res.* **2002**, *12*, 311; b) L. A. Ridnour, D. D. Thomas, S. Donzelli, M. G. Espey, D. D. Roberts, D. A. Wink, J. S. Isenberg, Antioxid. *Redox Signaling* **2006**, *8*, 1329.

[4] A. W. Carpenter, M. H. Schoenfisch, *Chem. Soc. Rev.* **2012**, *41*, 3742.

[5] L. J. Chen, Q. J. He, M. Y. Lei, L. W. Xiong, K. Shi, L. W. Tan, Z. K. Jin, T. F. Wang, Z. Y. Qian, *ACS Appl. Mater. Interfaces* **2017**, *9*, 36473.

[6] S. M. Yu, G. W. Li, R. Liu, D. Ma, W. Xue, *Adv. Funct. Mater.* **2018**, *28*,1707440.

[7] a) L. A. Tai, Y. C. Wang, C. S. Yang, *Nitric Oxide* **2010**, *23*, 60; b) V. Kumar, S. Y. Hong, A. E. Maciag, J. E. Saavedra, D. H. Adamson, R. K. Prud'homme, L. K. Keefer, . Chakrapani, *Mol. Pharm.* **2010**, *7*, 291; c) W. P. Fan, N. Lu, P. Huang, Y. Liu, Z. Yang, S. Wang, G. C. Yu, Y. J. Liu, J. K. Hu, Q. J. He, J. L. Qu, T. F. Wang, X. Y. Chen, *Angew. Chem. Int. Ed.* **2017**, *56*, 1229.

[8] a) D. L. H. Williams, *Acc. Chem. Res.* **1999**, *32*, 869; b) S. P. Nichols, W. L. Storm, A. Koh, M. H. Schoenfisch, *Adv. Drug Deliver. Rev.* **2012**, *64*, 1177; c) J. S. Xu, F. Zeng, H. Wu, C. P. Hu, C. M. Yu, S. Z. Wu, *Small* **2014**, *10*, 3750.

[9] a) M. J. Rose, P. K. Mascharak, *Coord. Chem. Rev.* **2008**, *252*, 2093; b) N. L. Fry, P. K. Mascharak, *Acc. Chem. Res.* **2011**, *44*, 289.

[10] a) P. C. Ford, *Nitric Oxide* **2013**, *34*, 56; b) J. Fan, Q. J. He, Y. Liu, F. W. Zhang, X. Y. Yang, Z. Wang, N. Lu, W, P. Fan, L. Lin, G. Niu, N. Y. He, J. B. Song, X. Y. Chen, *ACS Appl. Mater. Interfaces* **2016**, *8*, 13804; c) P. G. Wang, M. Xian, X. P. Tang, X. J. Wu, Z. Wen, T. W. Cai, A. J. Janczuk, *Chem. Rev.* **2002**, *102*, 1091.

[11] a) S. S. Lucky, K. C. Soo, Y. Zhang, *Chem. Rev.* **2015**, *115*, 1990; b) J. Hu, Y. Tang, A. H. Elmenoufy, H. B. Xu, Z. Cheng, X. L. Yang, *Small* **2015**, *11*, 5860.

[12] a) Z. G. Yi, X. L. Li, Z. L. Xue, X. Xiao, W. Lu, H. Peng, H. R. Liu, S. J. Zeng, J. H. Hao, *Adv. Funct. Mater.* **2015**, *25*, 7119; b) S. J. Zeng, Z. G. Yi, W. Lu, C. Qian, H. B. Wang, L. Rao, T. M. Zeng, H. R. Liu, B. Fei, J. H. Hao, *Adv. Funct. Mater.* **2014**, *24,* 4051; c) X. M. Li, Z. Z. Guo, T. C. Zhao, Y. Lu, L. Zhou, D. Y. Zhao, F. Zhang, *Angew. Chem. Int. Ed.* **2016**, *55*, 2464; d) Q. S.

Chen, X. J. Xie, B. Huang, L. L. Liang, S. Y. Han, Z. G. Yi, Y. Wang, Y. Li, D. Y. Fan, L. Huang, X. G. Liu, *Angew. Chem. Int. Ed.* **2017**, *56*, 7605; e) Y. S. Liu, D. T. Tu, H. M. Zhu, R. F. Li, W. Q. Luo, X. Y. Chen, *Adv. Mater.* **2010**, *22*, 3266.

[13] a) X. Zhang, G. Tian, W. Y. Yin, L. M. Wang, X. P. Zheng, L. Yan, J. X. Li, H. R. Su, C. Y. Chen, Z. J. Gu, Y. L. Zhao. *Adv. Funct. Mater.* **2015**, *25*, 3049; b) L. J. Tan, R. Huang, X. Q. Li, S. P. Liu, Y. M. Shen, *Acta Biomater.* **2017**, *57*, 498; c) C. X. Li, J. W. Shen, J. F. Yang, J. Yan, H. J. Yu, J. Liu, *Part. Part. Syst. Charact.* **2018**, *35*, 1700281.

[14] a) A. Kamkaew, F. Chen, Y. H. Zhan, R. L. Majewski, W. B. Cai, *ACS Nano* **2016**, *10*, 3918; b) L. Song, X. H. Lin, X. R. Song, S. Chen, X. F. Chen, J. Li, H. H. Yang, *Nanoscale* **2017**, *9*, 2718; c) D. J. Naczynski, C. Sun, S. Tiirkcan, C. Jenkins, A. L. Koh, D. Ikeda, G. Pratx, L. Xing, *Nano Lett.* **2015**, *15*, 96.

[15] W. P. Fan, W. B. Bu, Z. Zhang, B. Shen, H. Zhang, Q. j. He, D. L. Ni, Z. W. Cui, K. L. Zhao, J. W. Bu, J. L. Du, J. N. Liu, J. L. Shi, *Angew. Chem. Int. Ed.* **2015**, *54*, 14026.

[16] a) H. G. Chen, G. D. Wang, Y. J. Chuang, Z. P. Zhen, X. Y. Chen, P. Biddinger, Z. L. Hao, F. Liu, B. Z. Shen, Z. W. Pan, J. Xie, *Nano Lett.* **2015**, *15*, 2249; b) K. Rothkamm, M. Lobrich, *Proc. Natl. Acad. Sci. USA* **2003**, *100*, 5057.

[17] J. Sun, X. J. Zhang, M. Broderick, H. Fein, *Sensors* **2003**, *3*, 276.

[18] S. B. OH, H. R. Park, Y. J. Jang, S. Y. Choi, T. G. Son, J. Lee, *Br. J. Pharmacol.* **2013**, *168*, 421.

[19] Z. L. Xue, S. J. Zeng, J. H. Hao, *Biomaterials* **2018**, *171*, 153.

[20] F. Chen, S. J. Zhang, W. B. Bu, Y. Chen, Q. F. Xiao, J. N. Liu, H. Y. Xing, L. P. Zhou, W. J. Peng, J. L. Shi, *Chem. Eur. J.* **2012**, *18*, 7082.

[21] D. Seyferth, M. K. Gallagher, M. Cowie, *Organometallics* **1986**, *5*, 539.

Ultralow dosage Soft X-ray activated lanthanide scintillator-based light transducer for controllable NO release was developed for gas-sensitized tumor therapy *in vivo*.

Mingyang Jiang, Zhenluan Xue, Youbin Li, Hongrong Liu, Songjun Zeng, and Jianhua Hao**

Soft X-ray Activated Lanthanide Scintillator for Controllable NO Release and Gas-Sensitized Cancer Therapy